Hassan, W.; Reyes, J.; González, C.; Pallarés Rubio, FJ.; Spinel, J. (2021). Seismic vulnerability and resilience of steel-reinforced concrete (SRC) composite column buildings with non-seismic details. Engineering Structures. 244:1-14. https://doi.org/10.1016/j.engstruct.2021.112810

SEISMIC VULNERABILITY AND RESILIENCE OF STEEL-REINFORCED CONCRETE (SRC) COMPOSITE COLUMN BUILDINGS WITH NON-SEISMIC DETAILS

ABSTRACT

Prior to the enforcement of seismic details in the 1980s, older-type fully encased steel-reinforced concrete composite (SCR) columns were utilized in many buildings and bridges constructed in active seismic regions worldwide. However, there is serious lack of knowledge in the literature about the seismic behavior of older buildings' SRC composite columns with non-seismic details. Shear strength expressions, stiffness, backbone curves, nonlinear modeling parameters, and acceptance criteria for these columns are not available. A recent testing campaign (led by the first author) provided more test data to characterize the cyclic performance of SRC columns with non-seismic details. The current study has three primary objectives (1) suggesting some test-based nonlinear modeling parameters for SRC columns; (2) developing fragility, vulnerability and resilience functions for an older-type building with non-seismic details SRC columns; and (3) assessing ASCE 41-17 SRC column modeling recommendations by comparing prototype building performance, fragility, vulnerability and resilience functions obtained using test-based backbone curves and proposed nonlinear modeling parameters with those obtained using ASCE 41-17 SRC column criteria. The methodology used to establish economic vulnerability functions accounts for uncertainties in ground motion, structural response, damages and losses by means of Monte Carlo simulation techniques. The vulnerability functions for the structural, non-structural and content components of the prototype building are established. The results of this study demonstrate that the ASCE 41-17 criteria significantly underestimates the structural capacity and resilience and overestimates the seismic fragility and vulnerability of the system. The study shows that the ASCE 41-17 modeling criteria overestimates collapse probability by 30-50% for moderate ground shaking and by 5-15% for intense ground shaking.

Keywords: SRC columns, nonlinear modeling, vulnerability functions, existing buildings, fragility, probabilistic seismic risk assessment, non-ductile.

1. INTRODUCTION

Since the end of 20th century, national organizations and researchers have devoted great effort to develop techniques and databases to assess seismic vulnerability in large-scale regional domains such as urban areas, city centers or neighborhoods, with the aim to mitigate seismic damage and losses. For instance, European

Commission launched in 1999 the RISK-EU project to assess earthquake risk scenarios in different European towns: different proposals were stated to employ vulnerability models [1]. In the same line, PAGER project as a global building inventory from US Geological Survey [2], HAZUS-MH in USA [3], SYNER-G in Europe [4] or EMERCOM in the Russian Federation, are examples of contributions to deal with regional risk assessment using a database of building stock to enable loss estimates due to earthquakes. More recently, examples of works at a lower scale level are presented in [5], and [6], [7] and [8] for seismic vulnerability and buildings' damage patterns in Bucharest (Romania), and Senerchia (Italy), Scanno (Italy) and Seixal (Portugal), respectively. In all these approaches, buildings in the domain are classified by typologies that would exhibit similar seismic response, and usually these data are crossed with occupational classification to account for the influence of occupancy and casualties for overall assessments.

Descending one more scale level, reliable information about building seismic vulnerability is crucial to obtain building damage patterns in the domain under study, and this must be done for every structural system. Structural elements' seismic response characterization is fundamental in defining the systemic response of buildings to earthquakes. Depending on their response, structural and non-structural damage could lead to life and economic losses that may be unaffordable after a seismic event. Thus, the interest in developing realistic fragility and vulnerability functions for different structural systems based on test-calibrated component modeling is emerging rapidly. There are different methodologies for considering system vulnerability, ranging from empirical ([9], [10]) to analytical [11] or expert judgment. Recently, performance-based design methodologies have been coupled with vulnerability assessments to address the performance of specific structural systems. In this approach, structures are designed to meet a specific performance level while mitigating the losses in the aftermath of a seismic event. Reference [12] estimates vulnerability of blocks of buildings in the city of Osijek using both empirical and analytical methods in the field of seismic risk assessment and, in the same line, Haldar et al. [13] compare empirical and analytical methodologies. Yamín et al. [14] proposed a simplified approach to estimate the expected economic losses in terms of vulnerability functions for prototype buildings; in which developing fragility function is an intermediate step in the methodology. Pagnini et al. [15] discussed vulnerability assessment of old masonry buildings and fragility curves taking into account uncertainties and random limit states. Vulnerability and resilience functions permit to represent the economic losses as a function of different seismic hazard intensities, allowing not only the assessment of individual structures, but also the comparison of the behavior of distinct building typologies. The reader is referred to Singhal and Kiremidjian [16] for more information about probabilistic evaluation of seismic structural damage, where damage probability matrices and fragility curves are presented for different structural systems.

The existing building stock in many active seismic regions includes multiple seismically deficient concrete buildings that were constructed prior to enforcing seismic details in the 1980s. A large number of existing midrise and tall buildings and bridges utilize Steel-Reinforced Concrete (SRC) composite columns, which consist of structural steel sections embedded in concrete, that are not seismically detailed. This type of construction is quite common, especially in Asian countries. Literature reveals a serious lack of knowledge on the behavior of non-seismically detailed SRC composite columns subjected to simulated seismic loading conditions. Accordingly, performance-based earthquake nonlinear modeling is poorly informed by laboratory tests and nonlinear seismic design guidelines due to test scarcity. There is a small number of tests available to justify deriving seismic shear strength expressions and seismic backbone curves for cyclic nonlinear macro-modeling purposes of this class of columns. In addition, no information exists on the residual axial capacity of SRC composite columns following seismic shear or flexural failure due to premature test termination.

Existing experimental literature work has been primarily focused on the behavior of seismically detailed SRC columns. Lelkes and Gramblicka [17] tested 18 specimens to analyze the performance of slender SRC columns with high strength concrete. The specimens included completely and partially restrained SRC columns subjected to eccentric-axial compression loads. However, the seismic performance of the members was not addressed. Elnashai and Broderick [18] carried out tests to study the performance of partially encased composite beam-columns under seismic and axial loads. They constructed four identical specimens subjecting two of them to a pair of cyclic loading and performing five pseudo-dynamic tests to the remaining specimens. Two different detailing systems were compared in terms of test-seismic performance and economy, highlighting the good performance of SRC columns under earthquake loads when buckling is prevented. Campian et al. [19] presents experiments on composite steel-concrete columns with steel encased profile, showing that fully encased composite columns have high energy absorption capacities and good performances to cyclic loading. Ricles and Paboojian [20] studied six SRC column specimens to test lateral stiffness, transverse shear resistance, and degree of concrete confinement to achieve good ductility and effectiveness of shear studs in resisting lateral loading. Chen et al. [21] tested 26 SRC columns to study the seismic behavior influence parameters. They used three steel section shapes, changing the axial load ratio, longitudinal steel ratio, steel section ratio, embedded steel section length, and transverse steel ratio. It is noteworthy that most of the tested specimens in the aforementioned studies resembled modern construction practices. These studies highlighted the importance of the axial compression and hoop ratios on the seismic behavior of SRC columns, as well as the prevention of longitudinal bar buckling to preserve the integrity of the member. No recommendations for the backbone curves or performance acceptance criteria were made in these studies. Numerical models for the seismic performance of composite structures

have been receiving attention in the research community mainly for composite frames [22] (i.e. frames with reinforced concrete columns and steel beams), while structural systems with non-seismically detailed SRC columns have yet not been addressed. More recent studies on SRC columns include: reference [23], in which the authors simulate cumulative damage behavior in SRC specimens; reference [24], where authors aim to improve mechanical properties of this type of columns experimenting with new sections; or Montava et al. [25] that tested various steel sections in SRC joints. However, not many recent references can be found on the seismic vulnerability of this type of elements [26], even less for SRC elements built with non-seismic details.

In the United States, the American Concrete Institute (ACI) and the American Institute of Steel Construction (AISC) provide provisions for the design and analysis of SRC columns (ACI-318-14 [27], AISC 360-16 [28] and AISC 341-16 [29]). However, the calculated capacities of SRC columns are highly dependent on the method of calculation of the code. El-Tawil and Deierlein [30] conducted fiber section analyses to evaluate and compare the strength and ductility of SRC columns according to the design provisions of the ACI-318, AISC-LRFD Specification and the AISC Seismic Provisions. They analyzed nine SRC columns varying the ratio of structural steel to gross column area, the nominal compression strength of the concrete and the confinement of the member. They highlighted the large differences in the computed nominal strengths of the sections when using the ACI 318 and the AISC-LRFD code specifications and the effects of the strength of the concrete and the presence of axial compression on reducing the ductility of the sections. Moreover, the Seismic Evaluation and Retrofit of Existing Buildings Standard ASCE/SEI 41-17 [31] does not contain specific guidelines for SRC columns, leaving the retrofitting of existing structures with this type of columns to be modeled as steel sections ignoring the encasing concrete. This standard [31] considers that concrete encasement was often provided for fire protection rather than for strength or stiffness and typically lacks transverse reinforcement and proper confinement. However, the steel chapter of this Standard mentions that for components fully encased in concrete, calculation of the stiffness using full composite action shall be permitted if confining reinforcement is provided to allow the concrete to remain in place during an earthquake. A recent experimental campaign led by the first author of this study ([32], [33], [34], [35], [36], [37]) was conducted to characterize the seismic performance and suggest component modeling recommendations of SRC composite columns lacking seismic details mimicking pre-1980s typical SRC construction. Furthermore, even though SRC are widely used in pre-1980s buildings and bridges, studies about the seismic fragility and vulnerability for this type of structures and seismic loss estimation studies are completely absent in the literature.

The current study is an attempt to address some of these gaps by utilizing the test-based backbone curves and proposing some nonlinear modeling parameters for existing SRC columns based on this recent experimental campaign and, consequently, developing fragility, vulnerability and resilience functions for an older-type building with non-seismic details SRC columns. In addition, the study assesses the ASCE 41-17 SRC column nonlinear modeling recommendations by comparing prototype building performance fragility, vulnerability and resilience functions obtained using the suggested backbone curves to those obtained using ASCE 41-17 SRC column criteria.

2. RESEARCH SIGNIFICANCE

No research studies are currently available in the existing literature on evaluating the seismic risk in terms of fragility functions or vulnerability functions (economic losses) or building resilience (functional recovery) measures of SRC composite column buildings with non-seismic details. Thus, the objectives of this study are, based on suggested SRC test-based backbone curves [37], [40] and proposing some nonlinear modeling parameters for SRC columns: 1) development of fragility, vulnerability and resilience functions for an SRC composite columns building resembling older construction practices prior to enforcing seismic details, 2) assessing the suitability of ASCE/SEI 41-17 [31] nonlinear modeling recommendations for SRC composite columns via comparing seismic response, fragility, vulnerability and resilience functions of a building modeled using ASCE 41-17 and using test-based backbone modeling parameters. The framework for developing seismic vulnerability functions will be based on the methodology by Yamín et al. [14]. The results of this study can inform seismic assessment of existing building standards, performance-based seismic assessment methodologies, practicing engineers, peer-review panels, building officials, building owners and policy makers on the best practices to model SRC older buildings, the seismic probability of damage or collapse, and the cost of repair of such buildings.

3. TEST-BASED CYCLIC BACKBONE CURVES

Steel reinforced concrete composite columns comprise either a concrete encased hot-rolled steel section or a concrete filled hollow section of hot-rolled steel. They are usually used as a load-bearing members in a composite frame structure [38]. This type of columns is usually used for extra capacity with no increase in dimension for large unbraced lengths in tall building spaces, as transition columns between steel-concrete systems and for corrosion and fireproof protection in steel buildings. The current study focuses on encased hot-rolled SRC composite columns (Figure 1) mimicking older construction. According to ACI 318-63 [39], the composite column design equation does not differ from the current ACI 318-14 equation [27].

However, the main difference is the steel section ratio requirements, which is 5% to 9% A_c (where A_c is the gross concrete area) in the older code versus 1% to 3% A_c in ACI 318-14 code, and the longitudinal steel ratio, which is 2% to 3% A_c in the ACI 318-63 code instead of 1% to 2% A_c in the modern provisions.

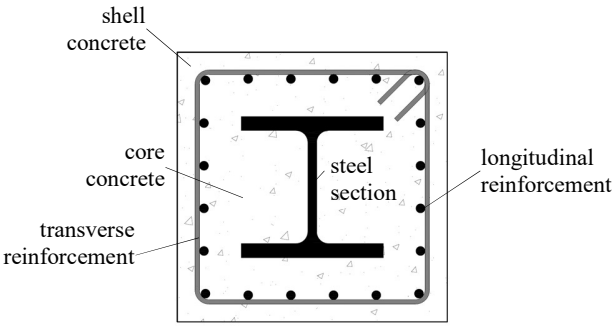

Figure 1. Typical SCR cross-section in older buildings; transverse reinforcement hook can be 90° or 135° depending on age of construction and country.

3.1 Previous Experimental work

A recent experimental campaign that aimed to characterize the seismic behavior and assist in developing backbone curves and nonlinear modeling recommendations for SRC composite columns with non-seismic details was carried out by Hassan and Farag ([32], [33], [34], [35], [36]). A 20-story prototype building mimicking older construction was used to obtain the demands on flexural-controlled exterior SRC columns. Fifteen single curvature large-scale SRC columns were constructed and tested cyclically [36] ; two of which (Specimens 5 and 6) are selected in the current study as reference specimens to present the experimental backbone curves ([40], [37]) and calibrate the prototype building nonlinear component model due to their relevance as will be discussed subsequently, with the details depicted in Figure 2 (a). The two-specimen subset's material and design parameters are shown in Table 1. The hoop spacing was selected in the test specimens ([33], [36]) as 75 mm to prevent shear failure and force the failure mode into flexure-tension mode, noting that the hoops have 90 degree non-seismic hooks so their confinement effect is limited. The specimens' cross-section was 250x250 mm and their effective height was 1000 mm. Their longitudinal reinforcement ratio, transverse reinforcement volumetric ratio and steel section area ratio were 1%, 1.34% and 5.4%, respectively. The specimens were tested under increasing quasi-static displacement amplitude reversals of three cycle per amplitude until failure ([33], [36]).

The specimens were tested under two different constant axial load ratios (ALR) of 15% and 80% (i.e. the ratio between axial load and the gross concrete section capacity based on cylinder compressive strength). These ratios represent the two extreme cases of tension-controlled and compression-controlled flexural

failure under typical demands of SRC buildings according to [33]. The specimens were designed by [36] according to ACI 318-63. More details about the adopted test specimens, test setup, testing protocol and the resulting response parameters can be found in [33] and [36].

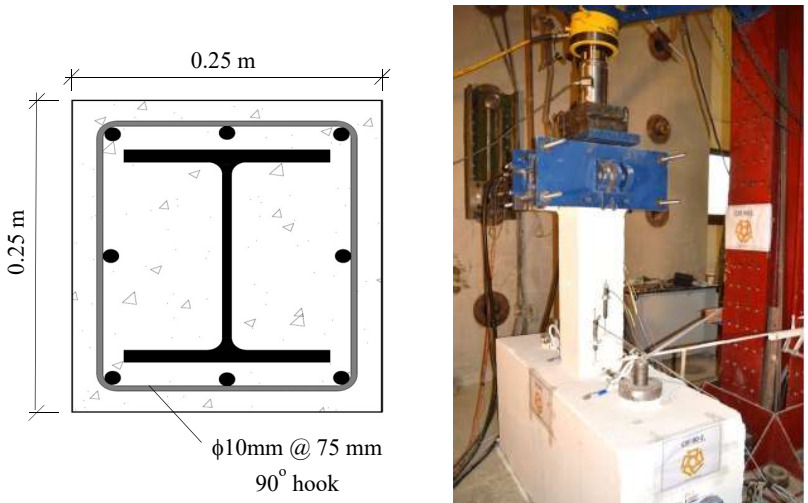

(a) (b)

Figure 2. (a) Typical specimen cross-section; and (b) Test set-up by Farag [36] and Farag and Hassan [33]

Table 1. Test specimen subset (from [36] and [33])

Specimen	f_c', MPa	Target failure mode	ALR	Specimen dimensions, m	Hoop spacing, mm	Steel section ratio, %	Reinforcement steel ratio, %
5	27.9	Flexural ten.-controlled	0.15	0.25×0.25×1.0	75.0	5.44	1.00
6	27.6	Flexural comp.-controlled	0.80	0.25×0.25×1.0	75.0	5.44	1.00

3.2 Experimental-based backbone curves

Section 7.6 of the ASCE/SEI 41-17 [31] provides an alternative procedure to derive the required parameters and acceptance criteria using the experimentally obtained cyclic response characteristics of a subassembly. According to this procedure, an idealized force-deformation curve shall be developed from the experimental data and the backbone obtained shall be plotted in a single quadrant. The envelope curves shall be drawn through each point of peak displacement during the first cycle of each increment of loading and then, the backbone should be approximated by a series of linear segments, drawn to form a multi-segmented curve. Figure 3 shows the hysteresis cycles of the two specimens tested by Farag and Hassan [33] and Farag [36]. Following the standard ASCE41-17 and using the hysteresis response of the specimens tested, backbone curves are developed for each of the specimens presented in Section 3.2 ([40], [37]). In Section 4.3,

nonlinear parameters of the selected computer models are calibrated against the experimental evidence. In the current study, additional nonlinear modeling parameters are suggested for implementation in building numerical simulations, such as axial load limits and energy degradation parameters as presented subsequently in Section 4.3.

The flexure-controlled specimens (Specimens 5 and 6) were selected from Farag and Hassan [33] and Farag [36] to calibrate the proposed the numerical model since they represent the most prevailing column failure mode in the prototype model, presented in the next section, after a failure mode and Axial Load Ratio (ALR) analysis of the building were performed. In the prototype building selected, which represents a typical high-rise building in high seismicity area (seismic demands of Los Angeles were used), flexural failure mode was observed in many columns exhibiting plastic hinging (since no considerations of strong-column weak-beam were given in older building code ACI 318-63 used to design the building).

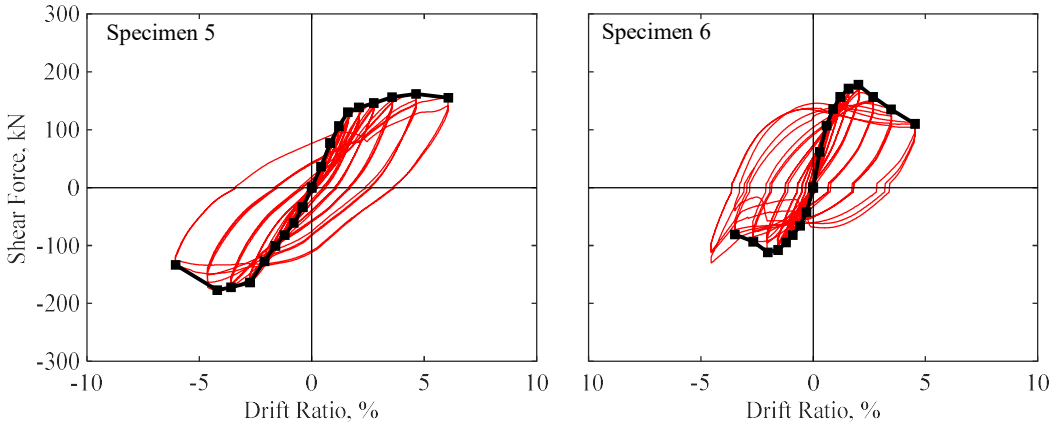

Figure 3. Test-based backbone curves [40], [37], for Farag [36] test specimen subset

4. BUILDING NUMERICAL MODELS

4.1 Design of prototype building

In this study, the seismic behavior of a prototype building with SRC columns mimicking older construction practices is addressed by developing and comparing the seismic responses of two different nonlinear models for the prototype building. The first model is based on the current seismic assessment nonlinear modeling recommendations in the ASCE/SEI 41-17, while the second model is developed based on test-derived backbone curves (Section 3, [40] [37]) and nonlinear parameters (Section 4.3). Besides literature search, several structural engineers were surveyed in active seismic regions in the US including San Francisco Bay Area and Greater Seattle Area to learn about the 1960s and 1970s practices in SRC buildings. The prototype

building considered in this study is originally adapted from the SAC steel project [41] and then redesigned to incorporate SRC in the perimeter frame columns, instead of steel columns, according to the ACI 318-63 and the 1964 International Building Code [42]. The loading information, building occupancy, floor plan characteristics, elevations and material properties were kept constant similar to the original SAC project for the new design. The prototype building selected is the 20-story Pre-Northridge model, designed as a typical office building in the city of Los Angeles (LA), California. The reader is referred to Gupta and Krawinkler [41] for more details about SAC project. The lateral force resisting system of this SAC building consists of perimeter moment resisting steel frames with a 120×100 ft plan area (Figure 4), a characteristic span length of 20 ft, a typical story height of 13 ft, and a first floor height of 18 ft, for a total height of 265 ft. The preliminary design of the SRC prototype building relied on period estimation using the period formulas for moment-resisting frame buildings proposed by Goel and Chopra [43], which provides rational limits for the fundamental period of buildings in California from 1971 (San Fernando earthquake) to 1994 (Northridge earthquake). For old designs like the one studied here, drift requirements were not included in that era, and the wind design drift were used (first author personal communication, S. Mahin, Oct. 2016), hence the final sections of the SRC columns were calibrated to achieve the measured periods for similar height structures as can be observed in
Figure 5a. Table 3 and
Figure 5b show the vibration periods of the designed building and its first mode shape, respectively.

The design process of the SRC prototype building features the following specifics. The concrete cylinder compressive strength is 4000 psi, resembling older construction's prevailing strength of SRC buildings obtained based on surveying several senior structural engineers. The SRC column prototype building is seismically designed according to UBC 1964 and ACI 318-63. Equivalent static lateral force analysis was performed using ETABS finite element platform to obtain design forces using the seismic demand of Los Angeles, based on the UBC 1964 provisions for Zone 3, the highest level at that time. The columns were designed using allowable stress design method based on ACI 318-63. The design shear strength of the columns was evaluated incorporating axial load ratio (ALR) from demand forces under the design loading conditions of the columns. The redesigned SRC column prototype building followed older details according to ACI 318-63 lacking modern design philosophies such as the strong column-weak beam concept and the transverse reinforcement of beam-column joints, the lack of confinement in the columns by using 90 degree hooks. During the design of the building SRC columns, it was attempted to keep the longitudinal and the steel section reinforcement ratios of the building SRC columns close as much as possible to test specimen ratios. However, some minor deviations occurred due to practical column design considerations vs. testing lab and similitude constraints of test specimens. Column transverse reinforcement spacing was selected in

building design based on the maximum limit permitted by ACI 318-63, which may be larger than that of the test specimen used to develop the backbone curve and calibrate the nonlinear modeling parameters due to scaling of test specimens and similitude and lab testing capabilities constraints. These two limitations are usually encountered in such numerical building modeling studies due to the limited test specimen availability. However, the impact of such limitations is thought to be minor in this study due to the slight variation of flexural reinforcement ratios from test specimens and the poor confinement of columns in both test specimen and prototype building SRC composite columns.

Older-type construction can lead to non-ductile structures very susceptible of presenting column shear failure and joint failure. Therefore, to evaluate the ultimate failure capacity of the columns, the shear strength of each member is compared against the required shear strength of the connection. The latter is calculated using Equation E3-6 of the AISC 341-16 [29], using the plastic moment of the column as the probable moment. The shear strength of the columns is calculated following the provisions for filled or encased composite members of the AISC 360-16 [28] because the maximum ALR calculated does not exceed 45%. The results of final SRC composite column design show that all columns are flexure-controlled, despite being designed with older codes. In the redesigned SRC prototype building, the SRC perimeter columns were classified into five cross sections (Figure 4); Table 2 shows each column type and the final sections used.

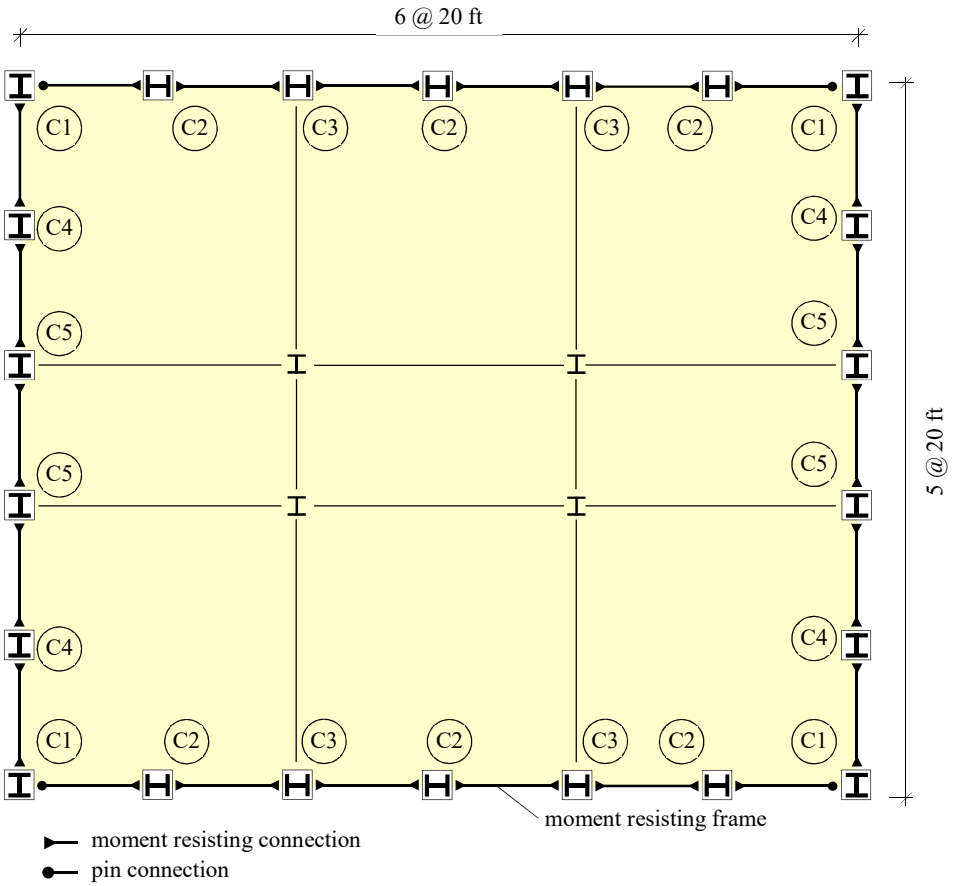

Figure 4. Floor plan of prototype building.

Table 2. Final design of SRC column cross-sections of prototype building.

Splice	Height, ft	C1	C2	C3	C4	C5
1	63	W14×211 (30×30 in) 8#11	W14×283 (32×32 in) 8#11	W14×257 (30×30 in) 8#11	W12×170 (25×25 in) 8#11	W14×283 (32×32 in) 8#11
2	102	W12×136 (25×25 in) 8#11	W14×159 (30×30 in) 8#11	W12×190 (25×25 in) 8#11	W12×170 (25×25 in) 8#11	W14×176 (30×30 in) 8#11
3	141	W12×106 (25×25 in) 8#11	W12×170 (25×25 in) 8#11	W12×170 (25×25 in) 8#11	W12×106 (25×25 in) 8#11	W12×170 (25×25 in) 8#11
4	180	W10×100 (20×20 in) 8#9	W12×106 (25×25 in) 8#11	W12×106 (25×25 in) 8#11	W12×106 (25×25 in) 8#11	W12×106 (25×25 in) 8#11
5	219	W10×77 (20×20 in) 8#9	W12×106 (25×25 in) 8#11	W10×100 (20×20 in) 8#9	W12×106 (25×25 in) 8#11	W12×106 (25×25 in) 8#11
6	265	W10×68 (20×20 in) 8#9	W10×77 (20×20 in) 8#9	W10×77 (20×20 in) 8#9	W10×112 (20×20 in) 8#9	W10×112 (20×20 in) 8#9

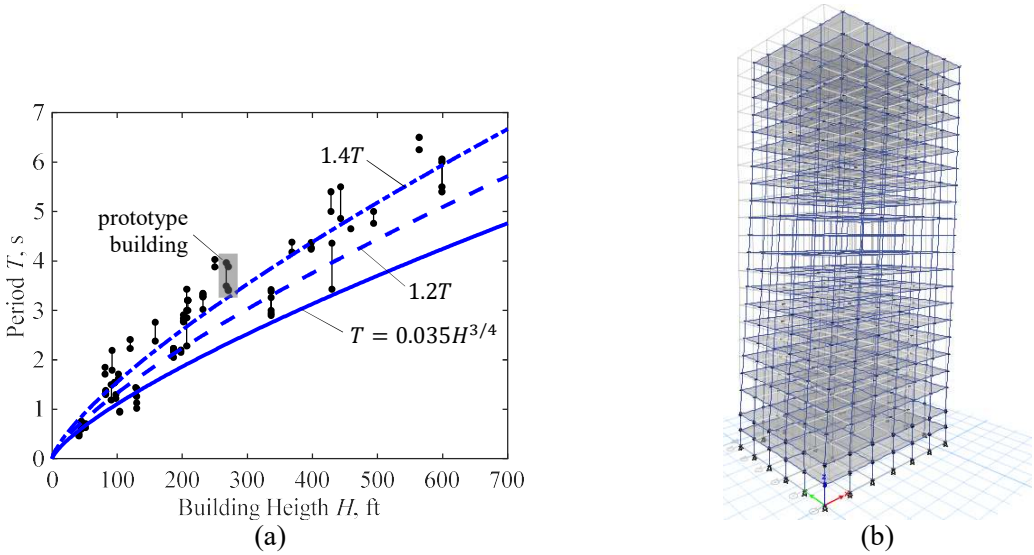

Figure 5. (a) Measured building periods versus height (from [43]); (b) Prototype building first mode deformed shape.

Table 3. Vibration periods of the prototype building

Mode	Vibration periods, s
1	3.54
2	3.51
3	2.25
4	1.30
5	1.26
6	0.83

4.2 Nonlinear modeling of prototype building

To evaluate the nonlinear seismic response of the prototype building, nonlinear response history analysis (RHA) is implemented in PERFORM-3D [44] under a suite of ground motions for the two proposed models. In the first building model (designated as Model 1), only the embedded steel sections are used to represent the nonlinear behavior of the columns following the recommendations of ASCE 41/SEI 41-17 for SRC column sections. Concrete encasement is considered to only provide protection against fire, and therefore, its resistance is neglected in the strength and resistance of the column. Hence, for the nonlinear component model, the columns of the moment resisting frames were modeled as beam-column steel elements with elastic sections in the middle of the column and concentrated nonlinear rotational springs at column ends using only the encased steel section of the SRC composite column. Nonlinear modeling parameters of column rotational springs were adopted from ASCE/SEI 41-17 for steel columns. In the second building

model (Model 2), columns are idealized as SRC composite sections using test-based nonlinear modeling parameters and backbone curves derived from experimental evidence. The effects of inelastic curvature along the span and rigid-body rotations associated with reinforcement bond-slip at column ends are lumped into plastic curvature acting along a plastic-hinge length. Other displacement components such as shear deformations are also considered in the elastic segment of both models. Axial-load dependent ductile limit and energy degradation parameters are taken into account (via Perform 3D model). For both models, the fiber cross-section analysis software XTRACT [45] is used to calculate parameters such as the curvature at first yield, the moment at spalling and the moment at first yield through the moment-curvature analysis of column sections. Nonlinear geometry effects were approximated by a standard P-Δ formulation for both gravity and moment frames and the floor diaphragms were assumed to be rigid.

4.3 Proposed stiffness, axial load limits and energy degradation parameters

In order to compute the energy parameters associated with the degrading hysteresis loops, energy dissipation and unloading stiffness for the composite column nonlinear building model (Model 2), the flexural-controlled test specimens described above are used as reference to calibrate the hysteretic response of SRC column components representing test specimens in PERFORM-3D and derive the corresponding energy parameters. Calibrated with respect to Specimen 5, the energy degradation parameters used in PERFORM-3D are shown in

Figure 6. A cantilever column model representing the test specimen, boundary conditions and the loading protocol, is implemented with the purpose of comparing the energy dissipation per cycle using a general cross section in PERFORM-3D. Table 4 and Figure 7 show a comparison between energy dissipation of Specimen 5 and the results from the numerical model for the first cycle of each displacement amplitude. It can be observed that the energy dissipated in the SRC component model (PF3D-Composite) matches the dissipated energy in the test for every displacement cycle. For comparison purposes, the same column is modeled using a steel only section with no energy degradation parameters (PF3D-Steel). It is also shown that this model underestimates hysteretic energy dissipation and that the steel column fails before reaching the maximum drift ratio observed in the test (Figure 7).

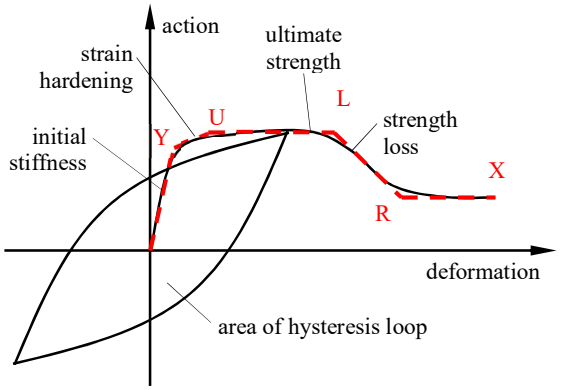

(a)

Hysteresis point	Energy Parameter
Y	0.99115
U	0.99045
L	0.98992
R	0.98698
X	0.30000

(b)

Figure 6. (a) Inelastic behavior implemented in the software (adopted from [46]), (b) Proposed SRC section calibrated energy degradation parameters.

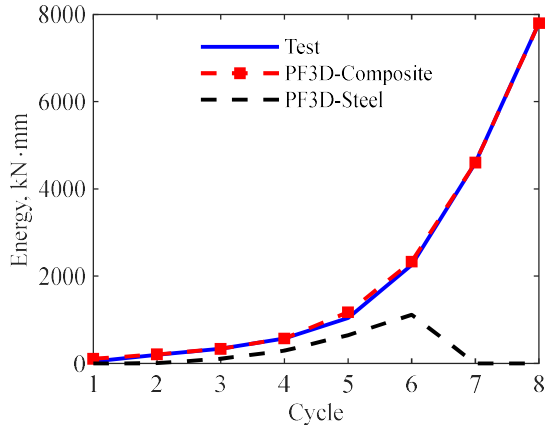

Figure 7. Hysteretic energy dissipation comparison of SRC nonlinear component model in Perform 3D and its test specimen counterpart. Steel section modeling option is also included for comparison.

Table 4. Energy dissipated per cycle for PERFORM-3D general section.

Cycle	Drift ratio, %	Dissipated Energy, kN·mm		
		Test	PF3D-Composite	PF3D-Steel
3	0.8	106.0	46.00	0.000
5	1.2	208.0	195.0	5.000
7	1.6	335.0	334.0	107.0
10	2.1	571.0	570.0	292.0
13	2.8	1174	1040	649.0
16	3.6	2334	2261	1116
19	4.7	4604	4595	-
22	6.1	7799	7799	-

Five different options for the estimation of the ultimate strength of the section are evaluated. The first option assumes a 15% increase in the yield strength due to strain hardening (1.15 F_y), the second and third options use the slopes from test (K_H Test) and backbone (K_H Backbone) until reaching the ultimate displacement, respectively; and the fourth and fifth options are based on the suggested slopes for steel (S_H Steel) and concrete (S_H Concrete) from the ASCE 41-17 (section 9.4.2.2.2 from ASCE 41-17 suggest using a 3% of the elastic slope for steel components, whereas section 10.3.1.2 suggest a maximum of 10% of the elastic slope for concrete elements). Results show that the ASCE 41-17 recommendations for concrete members give conservative and yet satisfactory estimations for both specimens (
Figure 8). The mean ALR of the building columns was 18% and the maximum experienced ALR was 38%. Therefore, Test Specimen 5 of Farag [36], (ALR of 15%, which is tension flexure-controlled) was deemed the most appropriate to calibrate the component model given the conditions of prototype building analysis. To validate the proposed numerical nonlinear component model for flexure-controlled SRC column, a comparison of the hysteresis force-drift responses of the SRC column Test Specimen 5 to that generated using the Perform 3D nonlinear component model for the specimen is presented in

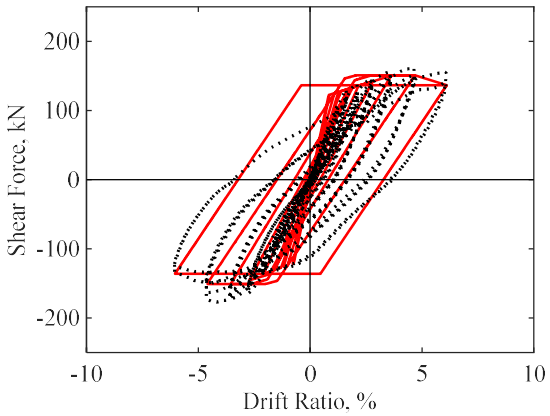

Figure 9.

The effect of axial load on ductile limit is also taken into account in the calibration of the model comparing four different ALR as the upper limit: 50%, 60%, 70% and 80%. The combination that better represents the test results takes 20% and 70% as the lower and upper ALR limits (
Figure 10). The ductile capacity of a column depends on the ALR, therefore, larger compression forces will lead to less ductile members. To account for this, PERFORM 3D allows to define the variation in rotation capacity at the ductile limit with axial force for steel columns but only in a simplified trilinear form of the proposed FEMA 356 model. This simplified form is a function of the cross-section area and the yield

strength, instead of the compression strength of the column. The actual proposed values were computed based on FEMA 356 equations and limits (FEMA 356 Table 5-6), and this simplification can be adopted with no practical loss of accuracy.

The confinement effect of transverse reinforcement has been well-studied by previous studies that found that transverse hoop confinement can prevent steel bar buckling, resist shear failure, and generate passive pressure on core concrete, which greatly improves the lateral load and ductility capacities [26]. Preventing bar buckling is crucial to maintain the integrity of the SRC member [20]. The limited confinement effect of the 90 degree hooked hoops has not been taken explicitly into consideration in the current study but rather implicitly, with the limitation mentioned in Section 4.1, by using lumped plasticity rotational spring model calibrated in Perform 3D and XTRACT for the nonlinear SRC component model against test Specimen 5 hysteretic response. Figure 9 shows the agreement of test and model responses proving the success of this approach which is typically followed in lumped plasticity nonlinear modeling.

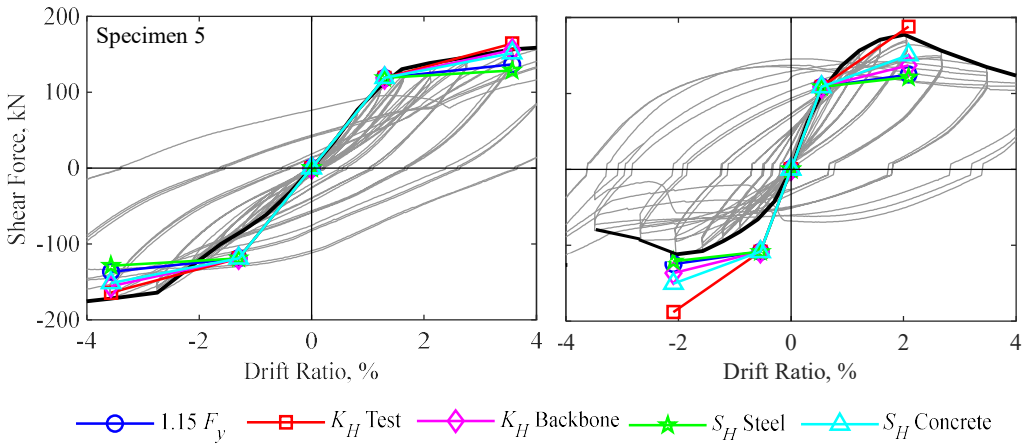

Figure 8. Proposed options for estimation of the ultimate strength of Farag [36] test specimens.

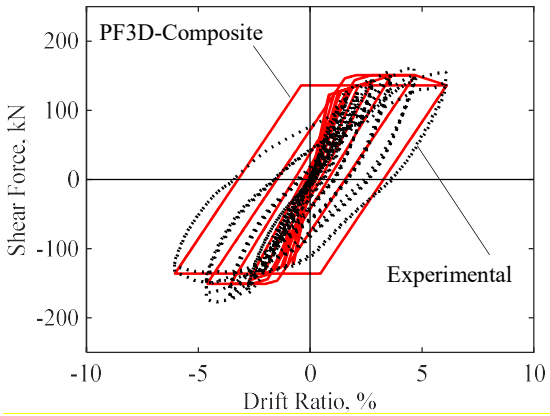

Figure 9. Comparison of the experimental vs. the proposed nonlinear component model (PF3D-Composite) hysteresis force-drift responses of the SRC column Farag [36] Test Specimen 5

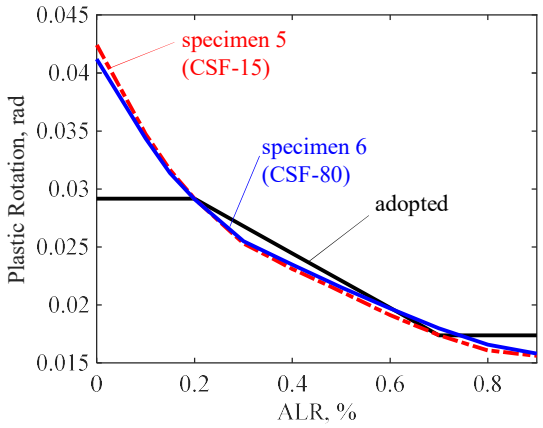

Figure 10. Effect of axial load on ductile limit of nonlinear SRC component model.

5. NONLINEAR RESPONSE HISTORY ANALYSIS

5.1 Ground Motion Selection

The suite of ground motion record used in the study is taken from the FEMA P695 methodology [47] for the collapse assessment of archetypical models appropriate using Incremental Dynamic Analysis (IDA). Two different record sets are addressed in the FEMA P695: a far-field (FF) and a near-field (NF) record set. The record sets of this methodology are selected due to their inherent characteristics that made them broadly applicable to a variety of structural systems and different location sites. The FF record set is both structure type and site hazard independent. Thus, the records do not depend on the period nor the site location of the structure [48]. Nonlinear response history analysis (RHA) under a suite of the 22 FF ground

404 motions shown in Table 5 was conducted for each of the building models. The main purpose of the analysis
405 was to develop fragility curves via incremental dynamic analysis; however, it is instructive to compare
406 building model responses under the effect of the ground motion suite at different intensity (scaling) levels
407 representing the service level or frequent earthquake, SLE, (corresponding to immediate occupancy
408 performance level), design-based/rare earthquake, DBE, (corresponding to life safety performance level)
409 and maximum considered earthquake/very rare earthquake, MCE, (corresponding to collapse prevention
410 performance level.) This comparison is useful to inform structural engineers and researchers about
411 quantified responses of this class of buildings at different performance levels for computer models using
412 steel sections (ASCE 41 recommendations) or SRC composite sections based on experimental backbone
413 curves. The results of this comparison are presented in next section. The seismic demand levels for the SLE,
414 DBE and MCE were taken from the target spectra for Los Angeles presented in report SAC/BD-00/25 [49]
415 for 50%, 10% and 2% probability of exceedance in 50 years, respectively. These target spectra, along with
416 the S_a values corresponding to the first vibration period of the prototype building, are shown in
417 Figure 11.
418
419

Table 5. Selected ground motions and main parameters (from [47])

ID	Magnitude	Year	Name	PGA_{max} / g	PGV_{max}, cm/s
1	6.7	1994	Northridge	0.52	63
2	6.7	1994	Northridge	0.48	45
3	7.1	1999	Duzce, Turkey	0.82	62
4	7.1	1999	Hector Mine	0.34	42
5	6.5	1979	Imperial Valley	0.35	33
6	6.5	1979	Imperial Valley	0.38	42
7	6.9	1995	Kobe, Japan	0.51	37
8	6.9	1995	Kobe, Japan	0.24	38
9	7.5	1999	Kocaeli, Turkey	0.36	59
10	7.5	1999	Kocaeli, Turkey	0.22	40
11	7.3	1992	Landers	0.24	52
12	7.3	1992	Landers	0.42	42
13	6.9	1989	Loma Prieta	0.53	35
14	6.9	1989	Loma Prieta	0.56	45
15	7.4	1990	Manjil, Iran	0.51	54
16	6.5	1987	Superstition Hills	0.36	46
17	6.5	1987	Superstition Hills	0.45	36
18	7	1992	Cape Mendocino	0.55	44
19	7.6	1999	Chi-Chi, Taiwan	0.44	115

20	7.6	1999	Chi-Chi, Taiwan	0.51	39
21	6.6	1971	San Fernando	0.21	19
22	6.5	1976	Friuli, Italy	0.35	31

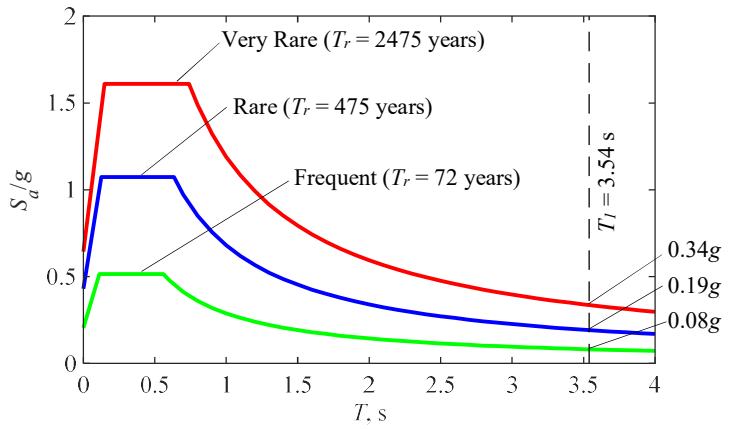

Figure 11. Target spectra for Los Angeles (adopted from [49])

5.2 Performance-based Deformation Response Comparison

Besides developing fragility, vulnerability and resilience functions for this type of buildings (SRC buildings with non-seismic details), it is informative to inspect some engineering demand parameters (EDPs) of the prototype building resulted from nonlinear dynamic analysis conducted at various intensity levels. This task enables numerical quantification of some key expected deformation EDPs at different seismic performance levels for this class of structures for performance-based assessment purposes. Furthermore, this investigation enables comparing the deformation EDP responses of the prototype building Model 1: code-based (ignoring concrete contribution) and those of Model 2: test-based SRC column numerical models, which will help judge the appropriateness of the current existing building seismic assessment standard ASCE/SEI 41-17 for this class of buildings.

Figure 12 plots the peak floor displacement responses over building height normalized by building height in the two principal directions of both prototype building models. These responses are the median peak floor displacement responses of the 22 ground motions in the selected suite. The responses are plotted for the three aforementioned performance levels, Immediate Occupancy, Life Safety and Collapse Prevention, defined based on the spectra and recurrence intervals of

Figure 11. The ground motion suite was scaled to match the target spectrum for every performance level as a part of the IDA intended for fragility assessment.

Figure 12 shows that peak floor displacement profiles using test-based or code-based nonlinear modeling parameters are quite close for IO and LS performance levels. However, it is clear that floor displacements

443 in the code-based model is significantly higher than those of the test-based SRC model in higher floors,
444 especially in *Y*-direction. The overestimation of the ASCE 41 of floor displacement reached 100% for the
445 peak roof displacement. The higher mode effects seem critical in exacerbating this effect.
446
447 In Figure 13, interstory drift ratio (IDR) profiles over building height are plotted for both building models
448 for the three selected performance levels. Again, the IDRs are the median responses to the 22 ground motion
449 suite. For the Frequent Earthquake (IO performance level), it seems that modeling option (code-based vs.
450 test-based) did not cause noticeable variation in IDR response, which was generally less than 1%. However,
451 for the LS performance level, which is implicitly the performance level intended by most building codes,
452 the ASCE 41 overestimation of IDR is quite clear, especially in the upper half of the building. The peak Y-
453 direction IDR was 2.5% for Model 1: code-based compared to 1.75% for Model 2: test-based, which
454 indicates about 43% IDR overestimation of ASCE 41 modeling recommendations. However, the ASCE 41
455 overestimation of IDR response is quite substantial for the CP level. Again, the higher mode effects seem
456 to exacerbate this effect in the upper one-third of the building. The maximum *X*-Dir IDR in the code-based
457 model, located at the 18^{th} story, was 4% compared to a 1.85% counterpart in the test-based model, a 216%
458 overestimation; however, if this 4% IDR is compared to the maximum IDR of test-based Model 2 of 2.8%,
459 located at the fourth story, then the ASCE 41 overestimation becomes about 43%. Similar comparisons can
460 be made for the *Y*-Dir CP performance level, which also yield about the same results. It is worth highlighting
461 that the maximum IDR level has changed in the code based Model 1 from level 18 to level 4 in the Model
462 2: test-based, suggesting the former is more influenced by higher mode effects. This indicates the substantial
463 conservatism of ASCE 41 recommendations for modeling SRC column buildings with non-seismic details,
464 especially at the Collapse Prevention performance level associated with intense ground shaking of PGA
465 0.34g.
466
467 It is also instructive to compare the Model 2: test-based results to the TBI 2017 [50] global acceptance
468 criteria for IDR at both SLE and CP performance levels. At the CP performance level, TBI 2017 [50]
469 prescribes an acceptance limit of 3% IDR for the mean response and 4.5% IDR for any single ground
470 motion response. The maximum IDR of Model 1: code-based significantly exceeded the 3% CP limit in
471 both *X* and *Y* directions, immediately triggering retrofitting needs for about the upper half of the building.
472 On the other hand, the maximum IDR for Model 2: test-based was 2.8%, less than the CP acceptance limit
473 at one story level, while the other stories' IDRs were significantly less than the 3% CP acceptance limit,
474 suggesting no need (or minimal need if any) for retrofit. Thus, the SRC building MCE performance,
475 although non-seismically detailed, actually satisfies the TBI CP acceptance criteria for new construction.

As for the SLE global IDR, TBI specifies 0.5% as acceptance criteria. Figure 12 shows that both test-based and ASCE 41-based models' IDR exceed that limit for several stories in both X and Y directions. The maximum peak IDR for Model 2, test-based model, was 1.2% which is more than twice the TBI acceptance limit for SLE IDR, indicating possible non-structural component damage over several stories under the frequent earthquake. The authors understand that these quantitative results may not represent every SRC building, but they can be representative of this class of midrise to high-rise regular plan building, which is quite common in SRC construction. This comparison, however, serves as a guide for practicing engineers, but does not substitute the need for through nonlinear response history analysis of other buildings using the suggested test-based backbone curves and proposed nonlinear modeling parameters.

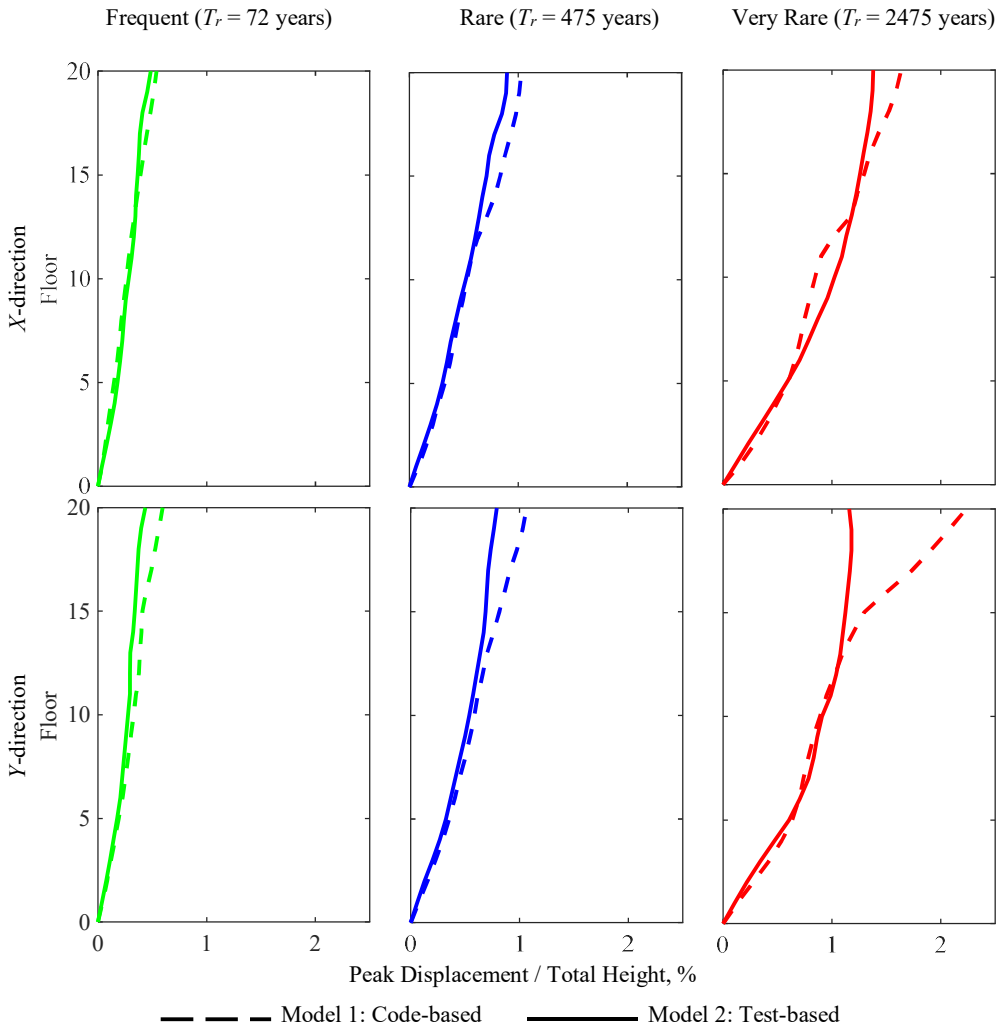

Figure 12. Median peak floor displacements for three seismic demand levels

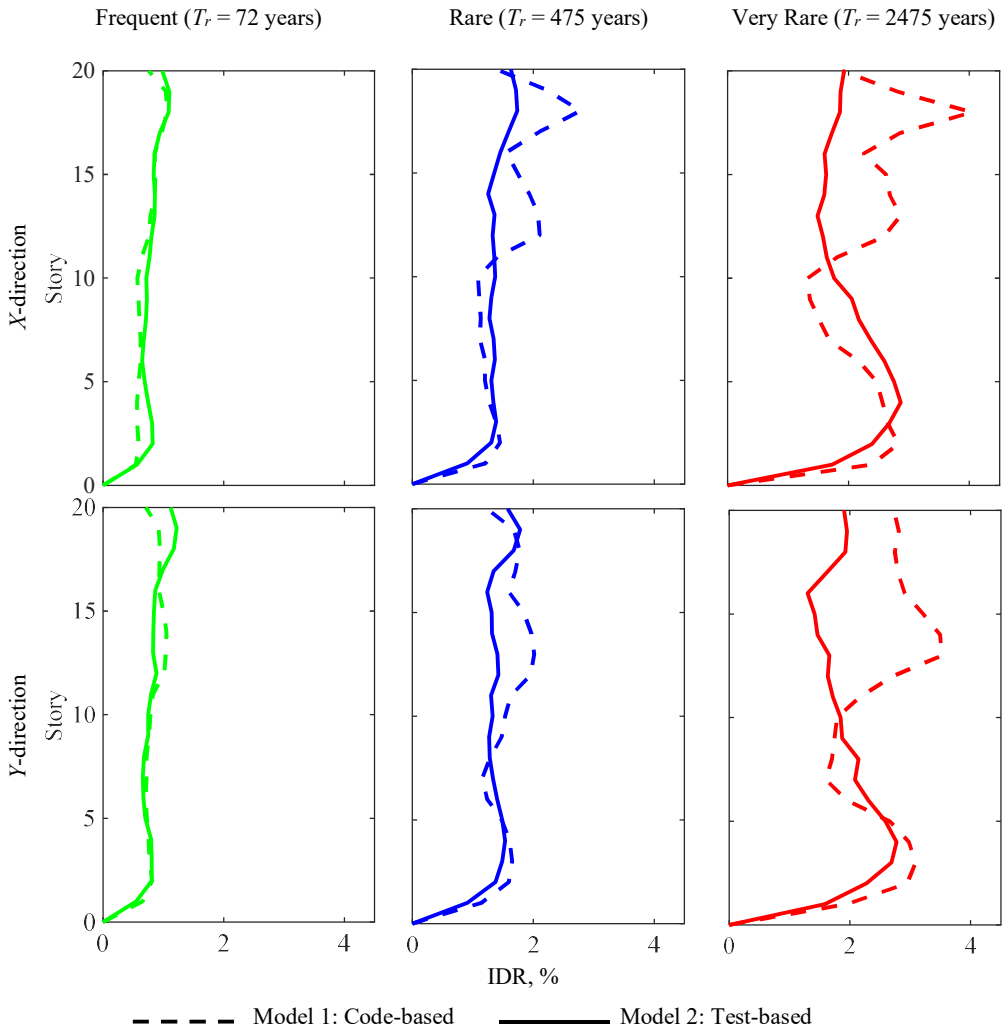

Figure 13. Median peak interstory drift ratios for three seismic demand levels

6. SEISMIC FRAGILITY, VULNERABILITY AND RESILIENCE ASSESSMENT

Fragility, vulnerability and resilience functions are the most common approaches used to relate the level of damage or loss for a given building typology and a hazard intensity parameter. Seismic fragility is typical established through a means of incremental dynamic analysis (IDA), which is developed in this study for both building models as will be described shortly. Seismic fragility of a structure can be defined as the probability of exceeding a given limit state while seismic vulnerability is the distribution of seismic loss, in this paper the economic loss, in the structure for a given seismic event. Seismic resilience involves estimation of the duration required to restore building function following earthquake damage. Yamín et al. [14] proposed a methodology to evaluate and integrate, in a consistent and rigorous way, the economic losses (vulnerability) as a function of the seismic hazard intensity for prototype building constructions. This

methodology has been followed herein, which also accounts for uncertainties in ground motion, structural response, damages and losses by means of Monte Carlo simulation techniques. For full details of the vulnerability function methodology, the reader is referred to Yamín et al. [14]. Almufti and Willford [51] methodolgy was used to assess functional recovery/seismic resilience. After choosing the building model under study and the seismic records, the aforementioned nonlinear RHA were conducted with varying seismic intensity. In this section, for every record and intensity, cost and full damage evaluations are performed. The cost estimation is obtained as a probability distribution function conducting all the analyses, adding direct and indirect losses, including uncertainties. The fragility functions provide the uncertainty damage measurement for the engineering demand parameter.

6.1 Incremental Dynamic Analysis Results

Incremental dynamic analysis (IDA) is conducted for the estimation of the probability of collapse as a function of a specified ground motion intensity [52]. The outcome of this analysis allows the estimation of a collapse fragility function and the probability of exceedance of critical engineering demand parameters at the ground motion intensities employed in the nonlinear model [53]. For the purpose of IDA of the two building models of this study, each 22-record ground motion suite was scaled up to 20 intensity levels for a total of 440 analyses per building model. The analysis was interrupted once collapse was presumed to occur. Collapse is assumed to occur either if the model presented numerical instability or if the horizontal maximum drift presented a dramatic increment with a low increase in the seismic intensity [14]. Engineering demand parameters (EDPs) such as interstory drift, maximum absolute story acceleration, and plastic hinge rotation demands are evaluated and stored for the subsequent vulnerability analysis. The IDA curves for the ASCE 41-based Model 1 and test-based Model 2 nonlinear models are presented in Figure 14. These curves relate the maximum interstory drift (the EDP parameter of interest) with the spectral acceleration at the fundamental period of the structure $S_a(T_1)$.

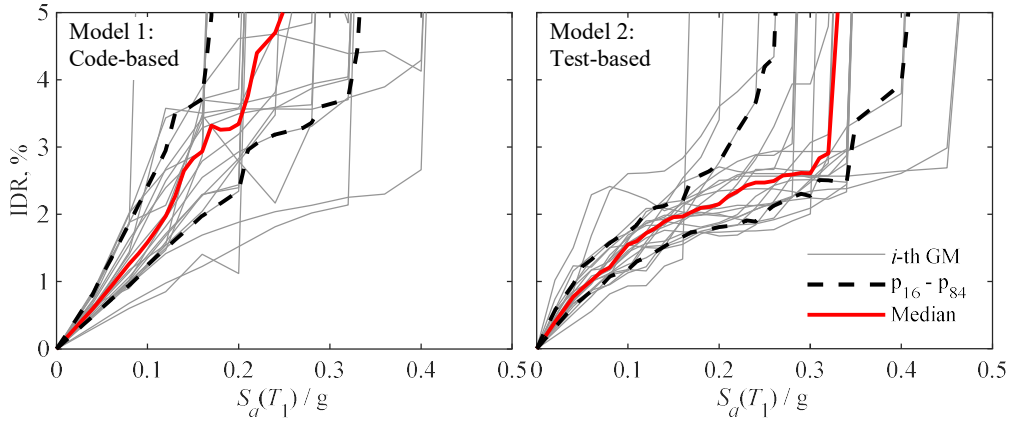

Figure 14. IDA curves for the nonlinear models

6.2 Seismic Fragility Functions

The outcomes from fragility assessments are shown as discrete values in the form of damage probability matrices or continuous values in the form of fragility curves. As discussed earlier, fragility curves relate the probability of exceeding a given damage state with an engineering demand parameter. In this paper, fragility curves were developed for the code-based (Model 1) and the test-based (Model 2) nonlinear modeling options using three different damage stages/performance levels corresponding to SLE, DBE and MCE events, respectively: Immediate Occupancy (IO), Life Safety (LS) and Collapse Prevention (CP). These limit states were selected due to their relevance to ASCE 41-17 acceptance criteria.

Figure 15 shows the results for the code-based (Model 1) and test-based (Model 2) nonlinear models, respectively. It is clear that modeling the columns based on the recommended ASCE 41-17 criteria (steel sections) lead to higher probability of damage/collapse of the building across all performance levels compared to modeling the columns as SRC composite sections using the proposed test-based backbone curves, despite the poor confinement of the SRC columns due to non-seismic hooks. In general, the fragility of the building is significantly overestimated if modeled using ASCE 41-17 recommendations leading to high damage/collapse probability at low ground motion intensity and consequently to unnecessary trigger of seismic retrofit at low seismicity. On the other hand, modeling option of Model 2, which is the proposed criteria, reflects more realistic and much lower fragility across all performance levels and shaking intensities, which may trigger seismic retrofit measures only in moderate to severe seismicity regions. For instance, it can be seen from Figure 15 that the fragility of Model 1 CP limit state under MCE is about 50% higher than that of Model 2 for low spectral accelerations (less than 0.1*g*), about 10%-30% higher than that of Model 2 for moderate spectral accelerations (0.1*g*-0.25*g*). Model 1 reached 100% MCE collapse probability at approximately 0.3*g* while Model 2 reached that percentage at higher than 0.5.

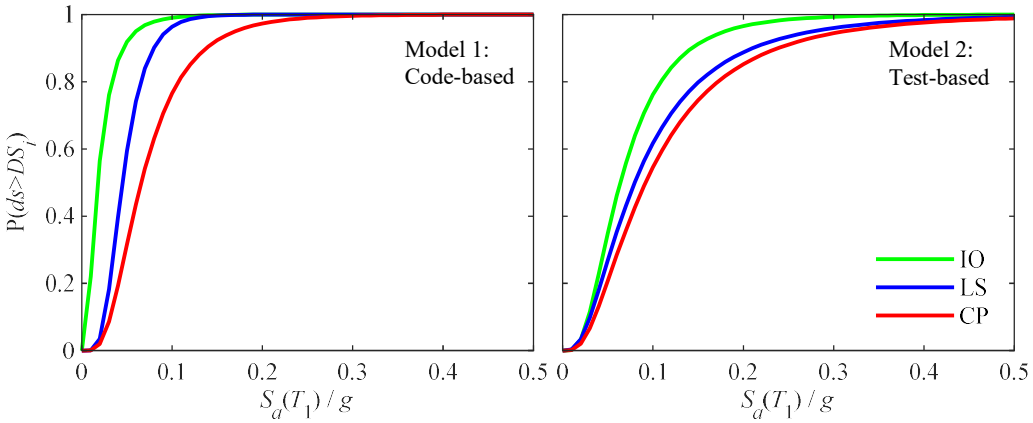

Figure 15. Fragility curves of the prototype building models

6.3 Seismic Vulnerability and Resilience Functions

Seismic vulnerability functions relate the probability of exceeding a chosen variable as a function of the seismic intensity (cost vs. spectral acceleration, in this paper), with their corresponding uncertainties. These functions represent the mean and variance of the costs for the whole range of the spectral acceleration under study. Building seismic resilience (functional recovery) is an estimate of the duration needed to re-establish building function following seismic damage. As mentioned above, Yamín et al. [14] is the methodology adopted herein to develop seismic vulnerability while the Almufti and Willford [51] methodolgy was used to assess functional recovery/resilience.

The software platform FUNVUL V1.0 [54], based on Yamín et al. [14] and available in the CAPRA webpage (https://ecapra.org), was used to generate the vulnerability functions for the structural, non-structural and content components. FUNVUL requires the estimation of the building replacement value, the downtime cost, the maximum duration of retrofit/intervention and downtime due to delays (resilience). For the first parameter, the RSMeans reference value for office building construction cost per square feet for Los Angeles was implemented. This value was modified by the historical cost index correspondent to the 2011-2018 period. The downtime cost (replacement value) per month was calculated through the reference costs of the National Building Cost Manual and applying a vacancy rate of 15%. Finally, the maximum time for seismic retrofit/intervention and downtime of the building was addressed following the methodology proposed in the REDi Rating System by Almufti and Wilford [51]. This methodology allows for the estimation of the time to re-occupy the building and to achieve functional recovery, as well as the time associated to the delays to initiation of repairs.

The parameters implemented in the program FUNVUL, in order to conduct the vulnerability assessment, are the following: (1) uncertainty in the dynamic response analysis $\beta_m = 0.5$; (2) number of iterations to account for uncertainties equal to 10; (3) a building replacement value of USD $48,723,840 and an interruption time replacement value equal to $638,520 USD/month; (4) maximum time for intervention of 1170 days (4.5 years) and a previous required time for intervention equivalent to 145 days; (5) maximum allowable residual drift to consider demolition equal to 1.5% [53]; (6) a lower intensity for no considered damage of 0 g/g and an intensity for building evacuation of 2 g/g; (7) factor for bidirectional damages equal to 1.3; (8) a 100% of building replacement value; and (9) four and nine member work crews for structural and non-structural repairs, respectively. More details in how the times for intervention and delays were estimated, as well as the calculation of the number of work crews can be found in Almufti and Willford [51]. These parameters allow to take into consideration aspects such as the uncertainty in the quality of construction, costs associated with the downtime of a building, the total replacement cost in case the

building needs to be demolished after a seismic event, and the costs associated to the labor work and repairs. The reader is referred to [14] for further details. The results for the cost model and vulnerability functions of the ASCE 41 code-based model (steel section only: Model 1) and the test-based model (SRC composite section: Model 2) are shown in Figure 16.

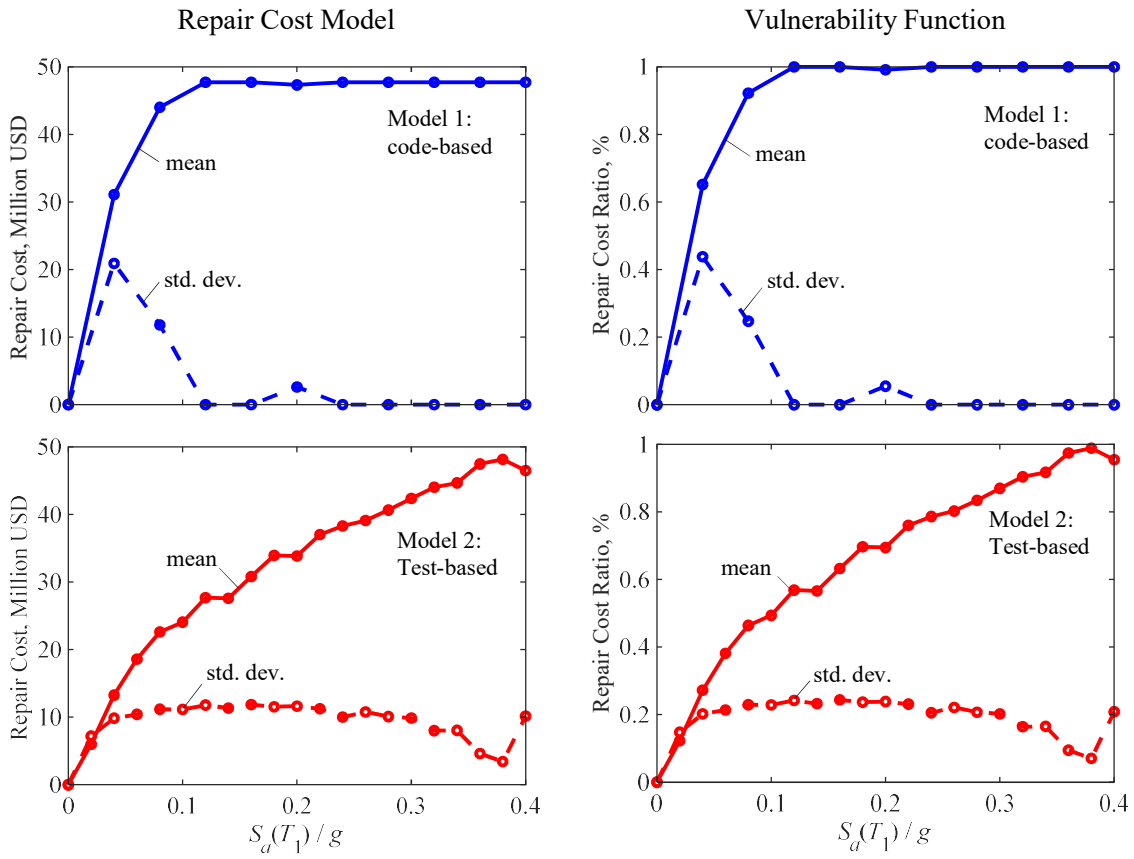

Figure 16. Vulnerability assessment results for the code-based and test-based models

As a way of comparison, Figure 17 illustrates the vulnerability functions for both models considered. It can be seen that the test-based model (Model 2) seems to be much less vulnerable due to its smoothness and lower increment in the mean damage ratio with the increase of intensity. Across all seismic intensity levels, Model 2 significantly exhibits less vulnerability in terms of cost of repair to the building original cost ratio. For instance, at low seismic intensity ($S_a < 0.1g$), Model 1 shows about twice the vulnerability ratio compared to Model 2. In the moderate seismic intensity range ($0.1 < S_a < 0.25$), Model 1 is more vulnerable than Model 2 by about 25% to 100%, and for high seismic intensity, Model 1 is more vulnerable than Model 2 by 10-25%. However, it is important to note that the two building models do not have the same fundamental period. These results indicate significant overestimation of seismic vulnerability and

underestimation of seismic resilience of ASCE 41-17 nonlinear modeling recommendations of older SRC column buildings. These modeling parameters need immediate update to reflect test-based cyclic backbone curves for SRC composite columns.

The resilience functions are shown in Figure 18. It is clear that the resilience of SRC buildings using Model 2 (test-based) under intense ground shaking is relatively low, incurring more than 20 week time until functional recovery. However, this resilience is much better than that of Model 1 (ASCE 41-based), which significantly underestimates the resilience of the system for moderate and intense seismic action, with the exception of very intense shaking which seems to incur slightly lower resilience for the SRC test-based model.

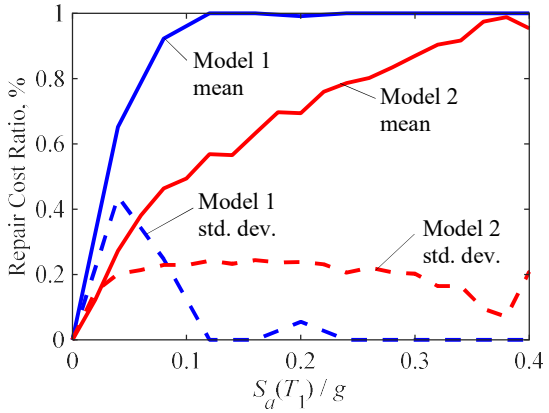

Figure 17. Vulnerability functions for Model 1 (steel, ASCE 41 code-based) and Model 2 (SRC, test-based).

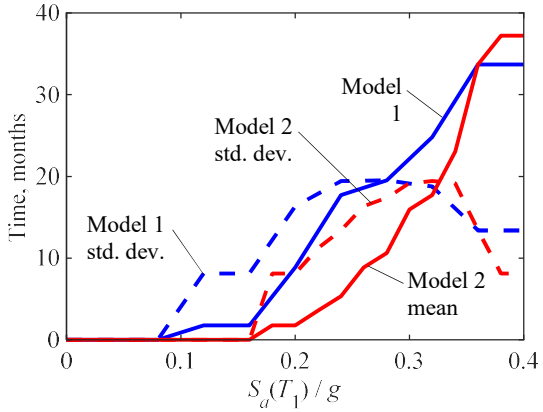

Figure 18. Resilience functions for Model 1 (steel, ASCE 41 code-based) and Model 2 (SRC, test-based).

7. CONCLUSIONS

In this study, existing gaps in the characterization of the seismic response of existing buildings with SRC composite columns with non-seismic details are addressed. Two different modeling approaches are used to evaluate the nonlinear behavior of a 20-story prototype building mimicking older SRC composite column construction practices with non-seismic details; using existing building assessment recommendations (ASCE/SEI 41-17 Standard) and experimental-based nonlinear modeling parameters. Subsequently, fragility and vulnerability functions in terms of economic losses and building resilience functions are developed to compare the expected behavior of the prototype building using the two different modeling approaches. An overview of the test specimens adopted and the test-based characterization of the prototype columns were presented followed by the design of the prototype buildings. The two nonlinear numerical models were constructed and analyzed under a suite of ground motions (based on ASCE 41-17 provisions vs. test-based modeling parameters.) The performance of the prototype model was evaluated at different intensity levels against the criteria of performance-based seismic design (PBSD) guidelines. Incremental dynamic analysis leading to fragility functions of the prototype building model using both modeling approaches are presented. Finally, the comparison between the two different modeling techniques is addressed by developing vulnerability curves in terms of economic losses as well as building resilience functions.

Results show that existing buildings with SRC composite columns could be less vulnerable than what is currently established in seismic assessment Standard (ASCE 41-17) under the design-based earthquake and maximum considered earthquake scenarios since ASCE 41 modeling recommendations for SRC composite column buildings were proven herein to be quite conservative leading to major underestimation of SRC building deformation capacity. As a result, the global deformation response of the evaluated SRC building based on the suggested test-based nonlinear modeling parameters satisfies the modern PBSD acceptance criteria (TBI-17) for the MCE scenario. However, the performance under the frequent earthquake did not satisfy modern PBSD acceptance criteria, with a maximum peak IDR of 1.2%. Across all seismic intensity levels, the test-based SRC building model significantly exhibits less vulnerability in terms of cost of repair to the building original cost ratio. In terms of building fragility, modeling the SRC columns based on the recommended ASCE 41-17 criteria leads to higher probability of damage/collapse of the building across all performance levels compared to building model with test-based modeled SRC columns. The fragility of the SRC building is significantly overestimated if modeled using ASCE 41-17 recommendations leading to unnecessary triggering of seismic retrofit even at low seismicity, while the test-based modeling is more realistic and it may trigger retrofit measures only at moderate to high seismic intensities. Moreover, the

ASCE 41-17 modeling recommendations for SRC buildings significantly lead to significant underestimation of building resilience compared to test-based nonlinear modeling. However, given the lack of experimental work on SRC columns resembling old construction practices, the findings are constrained to the limitations of the prototype building design, modeling and analysis as discussed in the manuscript and the details of the test specimens used to calibrate the numerical models. As more data becomes available, the model can be extended and refined to include different SRC column reinforcement and section ratios.

Overall, this study sets the base for a framework to evaluate the seismic behavior of existing buildings with SRC composite columns in terms of fragility, economic vulnerability and building resilience for broader building configurations. Future work may address buildings with SRC composite columns with different failure modes, such as shear-critical SRC columns, the development of fragility functions for other damage and performance levels, and refined backbone curves as more test data become available.

8. REFERENCES

[1] S. Lagomarsino and S. Giovinazzi, "Macroseismic and mechanical models for the vulnerability and damage assessment of current buildings," *Bull. Earthq. Eng.*, 2006, doi: 10.1007/s10518-006-9024-z.

[2] K. Jaiswal, D. Wald, and K. Porter, "A global building inventory for earthquake loss estimation and risk management," *Earthq. Spectra*, 2010, doi: 10.1193/1.3450316.

[3] Federal Emergency Management Agency, "Hazus–MH 2.1: Multi-hazard Loss Estimation Methodology," 2013.

[4] H. Crowley, M. Colombi, V. Silva, and N. Ahmad, "Systematic Seismic Vulnerability and Risk Analysis for Buildings, Lifeline Networks and Infrastructures Safety Gain - D3.1 - Fragility functions for common RC building types in Europe." European Commission, Joint Research Centre. European Research Project funded by FP7, Project No 244061, Seventh Framework Programme, 2011, doi: 10.1017/CBO9781107415324.004.

[5] I. Armaş, D. Toma-Danila, R. Ionescu, and A. Gavriş, "Vulnerability to Earthquake Hazard: Bucharest Case Study, Romania," *Int. J. Disaster Risk Sci.*, 2017, doi: 10.1007/s13753-017-0132-y.

[6] N. Chieffo and A. Formisano, "Geo-hazard-based approach for the estimation of seismic vulnerability and damage scenarios of the old city of senerchia (Avellino, Italy)," *Geosci.*, 2019, doi: 10.3390/geosciences9020059.

[7] D. Rapone, G. Brando, E. Spacone, and G. De Matteis, “Seismic vulnerability assessment of historic centers: description of a predictive method and application to the case study of scanno (Abruzzi, Italy),” *Int. J. Archit. Herit.*, 2018, doi: 10.1080/15583058.2018.1503373.

[8] T. M. Ferreira, R. Vicente, J. A. R. Mendes da Silva, H. Varum, and A. Costa, “Seismic vulnerability assessment of historical urban centres: Case study of the old city centre in Seixal, Portugal,” *Bull. Earthq. Eng.*, 2013, doi: 10.1007/s10518-013-9447-2.

[9] T. Rossetto and A. Elnashai, “Derivation of vulnerability functions for European-type RC structures based on observational data,” *Eng. Struct.*, 2003, doi: 10.1016/S0141-0296(03)00060-9.

[10] T. Rossetto, I. Ioannou, D. Grant, and T. Maqsood, “Guidelines for the empirical vulnerability assessment,” *GEM Tech. Rep.*, 2014, doi: 10.13117/ GEM.VULN-MOD.TR2014.11.

[11] D. D’Ayala *et al.*, “Guidelines for Analytical Vulnerability Assessment - Low/Mid-Rise,” *GEM Tech. Rep.*, vol. 08, p. 162, 2013, doi: 10.13117/GEM.VULN-MOD.TR2014.12.

[12] G. Pavić, B. Bulajić, and M. Hadzima-Nyarko, “The vulnerability of buildings from the osijek database,” *Front. Built Environ.*, 2019, doi: 10.3389/fbuil.2019.00066.

[13] P. Haldar, Y. Singh, D. H. Lang, and D. K. Paul, “Comparison of seismic risk assessment based on macroseismic intensity and spectrum approaches using ‘SeisVARA,’” *Soil Dyn. Earthq. Eng.*, 2013, doi: 10.1016/j.soildyn.2013.01.016.

[14] L. E. Yamin, A. Hurtado, R. Rincon, J. F. Dorado, and J. C. Reyes, “Probabilistic seismic vulnerability assessment of buildings in terms of economic losses,” *Eng. Struct.*, vol. 138, pp. 308–323, 2017, doi: 10.1016/j.engstruct.2017.02.013.

[15] L. C. Pagnini, R. Vicente, S. Lagomarsino, and H. Varum, “A mechanical model for the seismic vulnerability assessment of old masonry buildings,” *Earthq. Struct.*, 2011, doi: 10.12989/eas.2011.2.1.025.

[16] A. Singhal and A. S. Kiremidjian, “Method for Probabilistic Evaluation of Seismic Structural Damage,” *J. Struct. Eng.*, 1996, doi: 10.1061/(asce)0733-9445(1996)122:12(1459).

[17] A. Lelkes and S. Gramblicka, “Theoretical and experimental studies on composite steel - Concrete columns,” 2013, doi: 10.1016/j.proeng.2013.09.063.

[18] A. S. Elnashai and B. M. Broderick, “Seismic resistance of composite beam-columns in multi-storey structures. Part 1: Experimental studies,” *J. Constr. Steel Res.*, 1994, doi: 10.1016/0143-974X(94)90001-9.

[19] C. Campian, Z. Nagy, and M. Pop, “Behavior of fully encased steel-concrete composite columns subjected to monotonic and cyclic loading,” 2015, doi: 10.1016/j.proeng.2015.08.193.

[20] J. M. Ricles and S. D. Paboojian, “Seismic performance of steel-encased composite columns,” *J. Struct. Eng. (United States)*, 1994, doi: 10.1061/(ASCE)0733-9445(1994)120:8(2474).

[21] C. Chen, C. Wang, and H. Sun, “Experimental study on seismic behavior of full encased steel-concrete composite columns,” *J. Struct. Eng. (United States)*, 2014, doi: 10.1061/(ASCE)ST.1943-541X.0000951.

[22] S. S. Mehanny. and G. G. Deierlein, “Modeling of Assessment of Seismic Performance of Composite Frames with Reinforced Concrete Columns and Steel Beams.” The John A. Blume Earthquake Engineering Center, Department of Civil and Environmental Engineering, Stanford University, Stanford, 2000.

[23] L. Jiang, L. Jiang, and G. Bai, “Experimental Study on Cumulative Damage Behavior of Steel-Reinforced Concrete Columns,” *Adv. Civ. Eng.*, vol. 2020, 2020, doi: 10.1155/2020/5281725.

[24] Q. Wang, Q. Shi, W. Jiang, X. Zhang, W. Hou, and Y. Tian, “Experimental study on seismic behavior of steel reinforced concrete columns with new-type cross sections,” *Jianzhu Jiegou Xuebao/Journal Build. Struct.*, 2013.

[25] I. Montava, R. Irles, J. C. Pomares, and A. Gonzalez, “Experimental study of steel reinforced concrete (SRC) joints,” *Appl. Sci.*, 2019, doi: 10.3390/app9081528.

[26] M. M. A. Mostafa, T. Wu, X. Liu, and B. Fu, “The Composite Steel Reinforced Concrete Column Under Axial and Seismic Loads: A Review,” *Int. J. Steel Struct.*, 2019, doi: 10.1007/s13296-019-00257-9.

[27] American Concrete Institute, “Building Code Requirements for Structural Concrete (ACI 318-14).” American Concrete Institute, Farmington Hills, MI, 2014.

[28] American Intitute for Steel Construction, “Specification for Structural Steel Buildings, ANSI / AISC 360-16,” *Am. Inst. Steel Constr.*, 2016.

[29] American Institute of Steel Construction, “ANSI/AISC 341-16, Seismic Provisions for Structural Steel Buildings,” *Seism. Provisions Struct. Steel Build.*, 2016, doi: 111.

[30] S. El-Tawil and G. G. Deierlein, “Strength and ductility of concrete encased composite columns,” *J. Struct. Eng.*, 1999, doi: 10.1061/(ASCE)0733-9445(1999)125:9(1009).

[31] American Society of Civil Engineers, *ASCE Standard, ASCE/SEI, 41-17, seismic evaluation and retrofit of existing buildings*. Reston, Virginia, USA: American Society of Civil Engineers, 2017.

[32] M. G. Farag and W. Hassan, “Seismic Performance of Steel Reinforced Concrete Composite Columns,” *10th Pacific Conference on Earthquake Engineering*. Sydney, Australia, 2015.

[33] M. Farag and W. Hassan, “Seismic Performance of Flexural Controlled SRC Composite Columns in Existing Buildings,” 2017.

[34] W. Hassan and M. Farag, “Cyclic Performance Assessment of Seismically Deficient SRC Composite Columns,” *16th International Conference on Structural Faults and Repair, May 17-19*. Edinburgh, Scotland, UK, 2016.

748 [35] W. Hassan and M. Farag, “Seismic Performance of Shear Controlled SRC Composite Columns,” in
749 *16th World Conference on Earthquake Engineering, Jan 9-13*, 2017, pp. 2–5.
750 [36] M. Farag, “Seismic performance of steel-reinforced concrete composite columns of older and
751 modern construction,” Master’s Thesis. The American University in Cairo, 2018.
752 [37] W. M. Hassan, M. Farag, C. González, and J. C. Reyes, “Seismic performance of moment resisting
753 frames with SCR columns,” *8th National Congress on Seismic Engineering*. Barranquilla,
754 Colombia, 2017.
755 [38] Architectural Institute of Japan, “AIJ Standards for Calculation of Steel Reinforced Concrete
756 Structures.” Architectural Institute of Japan, Tokyo, 1987.
757 [39] American Concrete Institute, “Building Code Requirements for Structural Concrete (ACI 318-63).”
758 American Concrete Institute, Detroit, MI, 1963.
759 [40] C. D. P. Gonzalez Dueñas, “Seismic vulnerability of existing buildings with steel reinforced
760 concrete (SRC) composite columns,” Universidad de los Andes, 2018.
761 [41] A. Gupta and H. Krawinkler, “Seismic Demands for Performance Evaluation of Steel Mmoment
762 Rresisting Frame Structures.” Blume Earthquake Engineering Center, Stanford University,
763 Stanford, CA, 1999.
764 [42] International Conference of Building Officials, “Uniform Building Code.” International Conference
765 of Building Officials, Pasadena, CA, 1964.
766 [43] R. K. Goel and A. K. Chopra, “Period Formulas for Moment-Resisting Freame Buildings,” *J. Struct.*
767 *Eng.*, vol. 06, pp. 1454–1461, 1997.
768 [44] Computers and Structures, “PERFORM-3D V5.0.1: Nonlinear Analysis and Performance
769 Assessment for 3D Structures.” Berkeley, CA, 2011.
770 [45] C. B. Chadwell and R. A. Imbsen, “XTRACT: A tool for axial force - Ultimate curvature
771 interactions,” 2004, doi: 10.1061/40700(2004)178.
772 [46] Computers and Structures, “PERFORM-3D: User Guide.” Computers and Structures, Inc.,
773 Berkeley, CA, 2006.
774 [47] Federal Emergency Management Agency, “FEMA P695: Quantification of building seismic
775 performance factors,” *Fema P695*. Washington, DC, 2009.
776 [48] American Society of Civil Engineers, “ASCE Standard, ASCE/SEI 7-05, Minimum Design Loads
777 for Buildings and Other Structures.” American Society of Civil Engineers, Reston, VA, 2006.
778 [49] K. Lee and D. A. Foutch, “Performance Prediction and Evaluation of Steel Special Moment Frames
779 for Seismic Loads, Report No. SAC/BD-00-25.” SAC Joint Venture, 2000.
780 [50] Pacific Earthquake Engineering Center, “Guidelines for Performance-Based Seismic Design of Tall
781 Buildings,” *PEER Rep. 2017/06*, p. 147, 2017.

782 [51] I. Almufti and M. Willford, “REDi ™ Rating System: Resilience-based Earthquake Design Initiative
783 for the Next Generation of Buildings.” Arup Group, 2013.
784 [52] D. Vamvatsikos and C. Allin Cornell, “Incremental dynamic analysis,” *Earthq. Eng. Struct. Dyn.*,
785 vol. 31, no. 3, pp. 491–514, 2002, doi: 10.1002/eqe.141.
786 [53] C. M. Ramirez and E. Miranda, “Significance of residual drifts in building earthquake loss
787 estimation,” *Earthq. Eng. Struct. Dyn.*, 2012, doi: 10.1002/eqe.2217.
788 [54] A. Hurtado, “FUNVUL-Components V1.0.0.” Unviersidad de los Andes, Bogotá, Colombia, 2018,
789 [Online]. Available: https://ecapra.org/.
790